

Effect of phosphoric acid treatment on the physical properties of zinc telluride thin films

A. K. Aqili^{a,*}, T. Abu-Omar^a, A. Y. Al-Reyahi^a, A. Shaheen^a, S. Al-Omari^a,
I. Alhagish^a

^a*Department of Physics, Faculty of Science, The Hashemite University, P.O. Box 330127, Zarqa, 13133 Jordan*

Zinc Telluride (ZnTe) films were prepared by the closed space sublimation (CSS) method. The effect of chemical treatments with concentrated phosphoric acid, on the optical, electric and structural properties of the films was studied. Zinc-blend structure of the polycrystalline nature of the films was confirmed by x-ray diffraction (XRD) spectra. The energy dispersive x-ray (EDX) shows an increase in Te ratio on the surface of the film as exposed to phosphoric acid. In addition, the dc electrical resistivity of the films was dropped considerably. The refractive index, thickness, and thickness irregularity of the films were determined by fitting of the optical transmittance spectra in the wavelength range 400 to 2500 nm. The effect, of treatment, on the optical parameters is also reported.

(Received November 9, 2022; Accepted February 7, 2023)

Keywords: ZnTe, Thin films, Optical properties, X-ray diffraction, Zinc compound, Semiconducting II-VI materials

1. Introduction

Polycrystalline compound semiconductors films of are considerable technological importance and play a major role in electronic devices. ZnTe is one of the group II-VI semiconductors having a wide range of applications such as green light emitting diodes [1,2] due to its excellent electrical and optical properties. ZnTe is a p-type semiconductor with a direct band gap of 2.26 eV and a zinc-blend structure [3,4]. In addition to that doped ZnTe is used as a buffer layer, between CdTe absorber and metallic contact, in CdTe/CdS solar cells [5]. Due to importance of ZnTe a variety of methods have been utilized for deposition including pulsed laser deposition [1,5], sputtering [6,7], thermal evaporation [8–12], electron beam [13,14], screen printing [15], electro-deposition [16], brush plated [17] and closed space sublimation [3,18–20]. It is obvious that the deposition method and post-treatment have a great effect on the physical properties of the films.

Among the deposition methods, the CSS method is an attractive method for the deposition of II-VI semiconductor films. This is due to a good quality film that can be achieved under moderate pressure [3] and comparatively fewer materials use. On the other hand, it was reported that [21] treating CdTe (which has a similar structure as ZnTe) with nitric-phosphoric acid can improve its electrical properties.

In this work, we prepared ZnTe films by closed space sublimation method and then immersed them in concentrated phosphoric acid for different time periods. The effect of immersion of these films, in phosphoric acid, on their optical, structural, and electrical properties were studied.

2. Experimental

High-purity ZnTe powder (99.99) was used as source material for the deposition of the films, by CSS method, on carefully cleaned ultra-white glass substrate. Detailed descriptions of the

* Corresponding author: akramaq@hu.edu.jo
<https://doi.org/10.15251/CL.2023.202.113>

deposition unit are given in reference [20]. The distance between the source material and substrate was fixed at 0.8 cm. After achieving a base pressure of 0.01 mbar the substrate temperature was raised to 400 °C and then the source temperature was gradually raised to 600 °C and kept at this temperature for 5 minutes. The source heater then turned off while the substrate was kept at the same deposition temperature for 30 minutes before switching off the substrate heater and allowing the system to cool down. Many films were deposited with the same parameters. After deposition, the films were immersed in concentrated phosphoric acid, at 30 °C, for different time periods as listed in table 1, then rinsed with distilled water and dried with dry nitrogen.

The optical transmittance, in the wavelength range from 400 to 2500 was recorded by Perkin -Elmer Lambda 19, UV-VIS-NIR spectrophotometer with UV-WinLab software. X-ray diffraction patterns, with Cu-K α radiation, were used to study the structure of the films. The composition of the films was determined by energy dispersive system (EDS) attached to SEM. The surface morphology of the films was studied by scanning electron microscopy (SEM). The resistivity of the films was measured as function of temperature.

3. Results and discussion

3.1. Surface analysis and composition

The EDS results show that the tellurium ratio increased from 65 wt.% for as deposited film to 69 wt.% for film immersed for 48 hours. The tellurium ratio in the films increases as immersion time increases, which indicates the formation of a tellurium rich surface. The scanning electron microscope images, as shown in Fig.1, show a smooth surface with randomly distributed small spherical crystalline on the surface. This is due to that the film surfaces are dense, smooth, and compact in nature. However, a higher density of crystallite structure appears in immersed films. It could be explained in terms of surface etching, i.e., revealing the inner structure of the film.

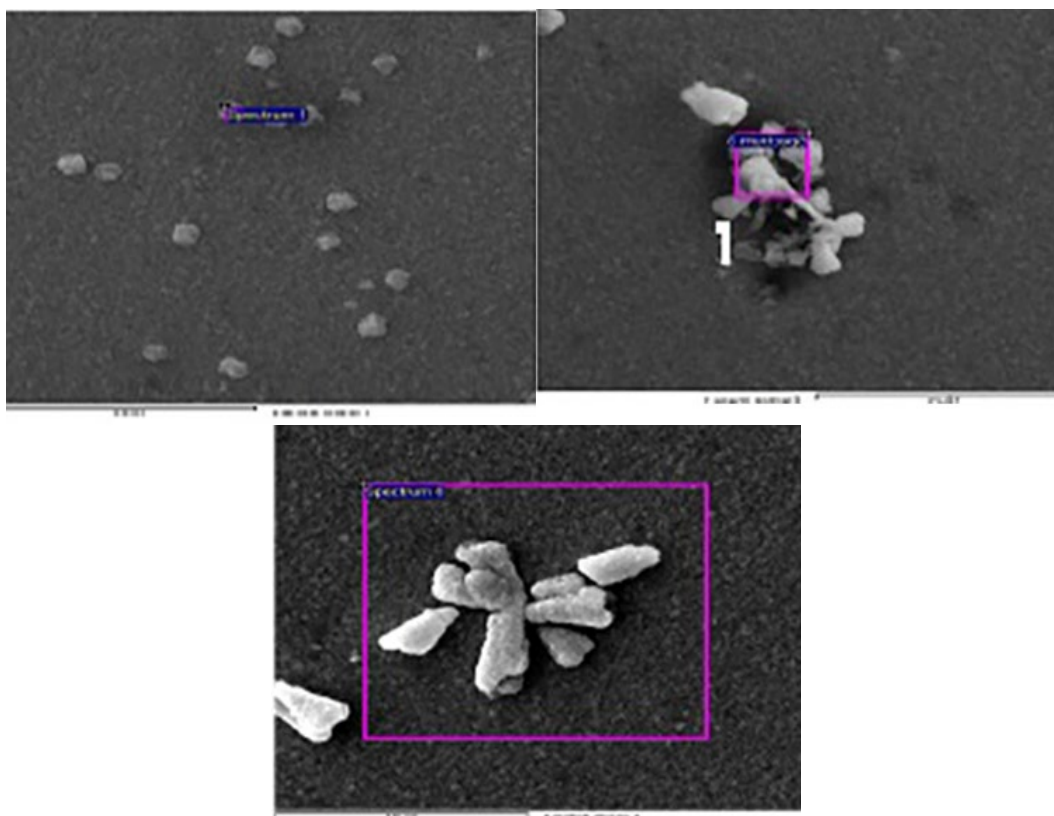


Fig. 1. Sem images of the films Z0 (left), Z24(middle), and Z48 (right).

3.2. Structural analysis

The x-ray diffraction patterns (Fig.2) show that all the ZnTe thin films (with or without immersion in phosphoric acid) prepared at the same substrate temperature and having almost the same thickness are present as a crystalline structure composed of cubic phase with a (111) preferred orientation. This structure and preferred orientation are common for ZnTe films deposited with a wide variety of techniques [1–12]. No notable changes in film structure or orientation were observed after immersion in phosphoric acid as in Fig.2.

Compared with standard JCPDS card No.15-0746, all ZnTe films exhibit a zinc blend structure with strong preferential (111) orientation. The (111) peak positions which are located at 2θ are 25.4198° , 25.3996° , 25.4196° , and 25.3991° for the films deposited at different immersion times, respectively.

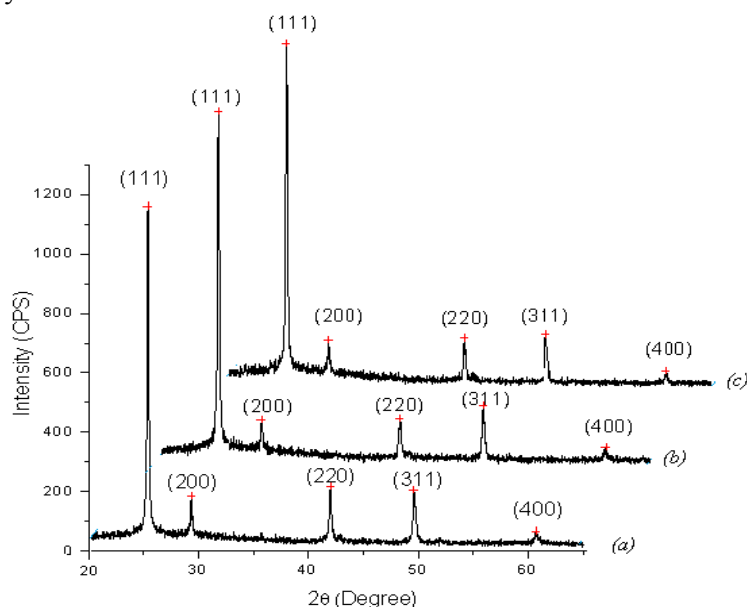


Fig. 2. Xrd pattern of the films Z0 (a), Z24(b) and Z48 (c).

The variation in crystalline size of the films was determined from the full width at half-maximum (FWHM) of the peak corresponding to the (111) plane using the Scherrer relation [1,4]

$$t = \frac{0.94\lambda}{B\cos\theta}$$

where t is the diameter of the crystalline particle, λ is the wavelength of the x-ray used (0.154 nm), B is the full width at half-maximum and θ is the scattering angle. The calculated crystalline size of the films is ~ 45 nm and a slight difference (~ 2 nm) observed in the crystalline size could be attributed to the small difference in the thickness of the film. The calculated crystalline size was larger than that reported by other deposition methods [1].

3.3. Electrical properties

The P-type conductivity of the films were verified by a well-known hot probe method. The room temperature resistivities for all films are listed in table 2. The resistivity of the as deposited films was very high $\sim 10^6 \Omega\text{-cm}$, which is close to that reported for undoped ZnTe [3] films. However, the resistivity has been dropped to $\sim 10^4 \Omega\text{-cm}$ for treated films. With no available literature related to the phosphoric acid treatment of ZnTe films (according to our knowledge), the reduction of resistivity by etching CdTe by phosphoric acid was reported by reference [21]. They reported that there is a decrease in the film's resistivity and a reduction in the effective bulk resistivity due to the formation of a Te-rich layer on the grain boundaries.

The linear relation between the current and voltage which confirm ohmic contact junction with ZnTe film and silver paste used to measure the conductivity. Moreover, this linear relation indicates ohmic contact between the film surface and metallic contact which could be useful for the application of ZnTe as a buffer layer between CdTe absorption layer and metallic contact for CdTe based solar cells.

The dark conductivity activation energy ($E_a = E_F - E_v$) was obtained by linear fitting $\ln \sigma$ vs. $k_B T$, where k_B is the Boltzmann constant, E_F is the fermi energy level and E_v is the energy at the top of valance band. Fig. 3 shows the linear relation between $\ln \sigma$ and $1/k_B T$ and the electrical results are listed in Table1.

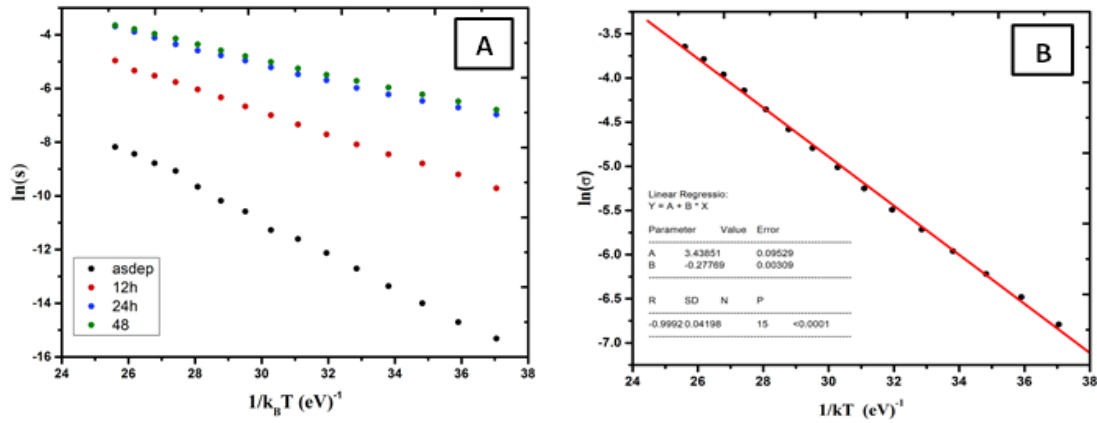


Fig. 3. plot of $\ln(\sigma)$ against $1/kT$ for all films (A).and Fitting of $\ln(\sigma)$ against $1/kT$ for film Z24 (B).

It clearly shows that the conductivity activation energy of the films was reduced from 0.64 eV to 0.26 eV indicating increase of hole concentration led to shift of fermi energy level closer to the valance band.

Table 1. The dc electrical resistivity of the as deposited and immersed ZnTe films.

Film number	Immersion time (hour)	Activation Energy E_a (eV)	Resistivity ρ ($\Omega.cm$)
Z0	0	0.64	1.26×10^6
Z12	12	0.30	1.29×10^3
Z24	24	0.28	4.07×10^4
Z48	48	0.26	2.19×10^4

3.4. Optical properties

The as deposited zinc telluride films were orange in color. The films lose their transparency as immersed in a phosphoric acid solution. This can be attributed to an increase in tellurium on the surfaces of the films.

Fig. 4. shows the transmittance spectra of as deposited as well as treated films along with transmittance spectra of 10 nm tellurium film, in order to compare the decrease of transmittance due to the increase of Te concentration in the films. It is obvious that the reduction of transmittance below 2000nm follows the same trend as tellurium film. The reduction of transmittance is attributed to the formation of Te excess layer on the film surface due to etching with phosphoric acid. The normal transmittance (T) for a system of thin film (of refractive index n and extinction coefficient k) on a transparent substrate (of refractive index n_s) surrounded by air and $k^2 \ll n^2$ can be written as [11,22]

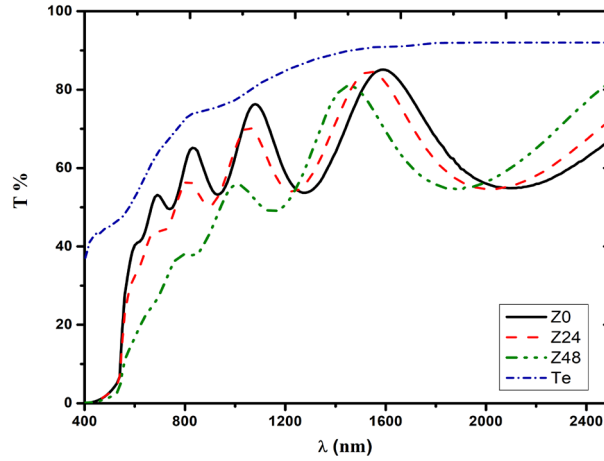


Fig. 4. Transmittance of prepared ZnTe films along with 10 nm Te film.

$$T = \frac{Ax}{B - Cx \cos(\phi) + Dx^2} \quad (1)$$

$$A = 16 (\text{Exp}[-0.5(2\pi\sigma/\lambda)^2(1-n)^2])^2 n_s n^2, B = (n+1)^3(n+n_s^2),$$

$$C = 2(n^2-1)(n_2^2-n_s^2)(\text{Exp}[-2(2\pi\sigma/\lambda)^2 n^2])$$

$$D = (n-1)^3(n-n_s^2)(\text{exp}[-2(2\pi\sigma/\lambda)^2 n_2^2])^2, \phi = 4\pi nd/\lambda, x = e^{-\alpha d}, \alpha = 4\pi k/\lambda$$

Here, λ is the incident photon wavelength, d is the film thickness, ϕ is the phase angle, α is the absorption coefficient and σ is the RMS height of surface roughness(irregularity). It was found that the refractive index of the ZnTe films obeys the simple classical dispersion relation for a single oscillator centered at wavelength λ_0 [11,12,22] and expressed by

$$n = \left(1 + \frac{(n_0^2 - 1)\lambda^2}{\lambda^2 - \lambda_0^2}\right)^{1/2}, \quad (2)$$

where n_0 is the infinite wavelength refractive index. The wavelength dependence of the absorption process is complicated, resulting from impurity, defects, or multi-phonon absorption [23]. Therefore, in case of low absorption coefficient, it may be expanded in a Taylor series around the photon energy far from absorption line. If only terms up to second degree are included (α varies slowly with λ), the relation for α can be expressed as:

$$\alpha = (c + g/\lambda + f/\lambda^2) + (e^{m+h\lambda}), \quad (3)$$

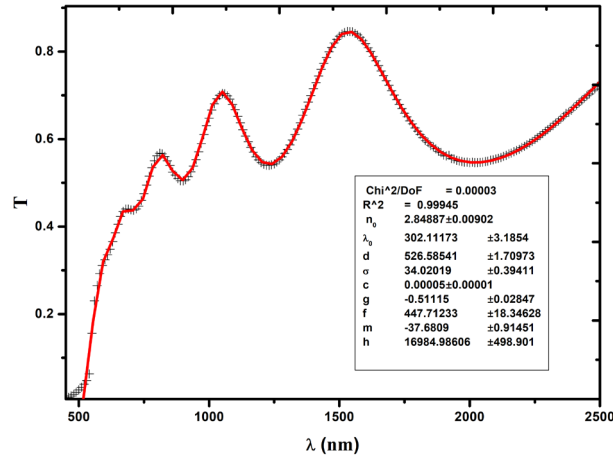


Fig. 5. Transmittance data of film Z24 along with fitting curve.

where c , g , f , m and h are fitting parameters. The second term in equation 3 is relating to Urbach's relation [24], which represents the absorption edge of an intrinsic semiconductor. While the first term is a polynomial approximation of the absorption coefficient resulting from impurity, defects, or multi-phonon absorption. Fig. 5 shows a good fitting in transparent and low absorption of wavelength region, using equation 1 and substitution equations 2 and 3 for n and α . consequently, the values of the thickness, thickness irregularity, and refractive index were obtained. However, the values of the absorption coefficient in the high absorption region were found by solving equation 1 after substituting the other parameters obtained from transmittance curve fitting.

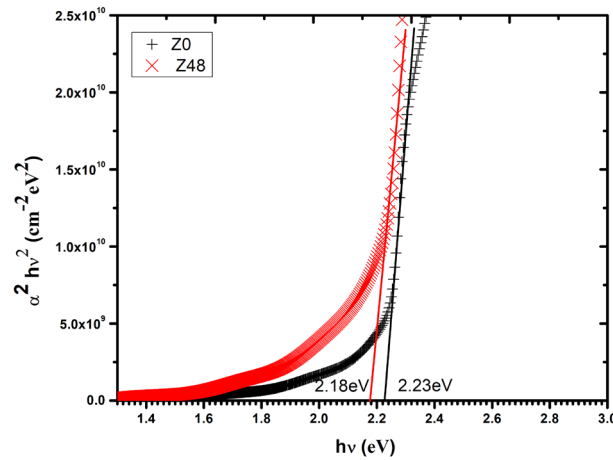


Fig.6. Plot of $\alpha^2 (h\nu)^2$ against photon energy ($h\nu$) for films Z0 and Z48.

For allowed direct transition, α varies with photon energy ($h\nu$) as the well-known dependence $\alpha \sim (h\nu - E_g)^{1/2}$. Near the absorption edge, the optical energy gap (E_g) is obtained by extrapolating $(\alpha)^2$ against the photon energy plot as in Fig.6. The fitting results along with optical energy gaps are listed in Table 2. No significant change in the surface roughness, which indicates that deposition conditions are more dominant and effective in films morphology rather than post-treatment and since all the films were prepared with the same deposition parameters there is no clear difference in surface roughness and the roughness is comparable with grain size deduced from x-ray results. The change in refractive index was clear as result of increasing in the films absorption. Furthermore, minor shift of optical energy gap was observed.

Table 2. Fitting results along with calculated optical band gap.

Film number	Thickness d (nm)	Thickness irregularity (nm)	Refractive index		Optical band gap E_g (eV)
			n_0	λ_0 (nm)	
Z0	563	29.3	2.77	288	2.23
Z12	420	28.6	2.70	330	2.22
Z24	526	34	2.82	302	2.20
Z48	500	31	2.83	293	2.18

4. Conclusions

Optical, electrical, and composition results insure the formation of Te rich layer by immersion ZnTe films in concentrated phosphoric acid solution at room temperature. The formation of Te rich surface led to increase the electrical conductivity of the films. No significant change in the structure of the film was observed, while the optical properties such as refractive index and optical energy band was slightly affected. The etching procedure was very slow, so it required a long time for small changes in the physical properties to be observed. The Increase of electrical conductivity with no drastic change in optical and structure of the films can attribute to application where heavily doped zinc telluride layer is required.

References

- [1] A. Erlacher, A. R. Lukaszew, H. Jaeger, B. Ullrich. Surface Science 600, 3762 (2006); <https://doi.org/10.1016/j.susc.2006.02.061>
- [2] F. J. Ochoa-Estrella, A. Vera-Marquina, I. Mejia, A. L. Leal-Cruz, M. Quevedo-López. J Mater Sci: Mater Electron. 29, 7629 (2018); <https://doi.org/10.1007/s10854-018-8755-3>
- [3] F. J. Ochoa-Estrella, A. Vera-Marquina, I. Mejia, A. L. Leal-Cruz, M. I. Pintor-Monroy M. Quevedo-López. J Mater Sci: Mater Electron. 29, 20623 (2018); <https://doi.org/10.1007/s10854-018-0200-0>
- [4] H. Singh, T. Singh, J. Sharma. ISSS J Micro Smart Syst. 7, 123 (2018); <https://doi.org/10.1007/s41683-018-0026-2>
- [5] L. Feng, L. Wu, Z. Lei, W. Li, Y. Cai, W. Cai, J. Zhang, Q. Luo, B. Li, J. Zheng. Thin Solid Films 515, 5792 (2007); <https://doi.org/10.1016/j.tsf.2006.12.122>
- [6] E. A. Rakhshani, S. Thomas. J Mater Sci . 48, 6386 (2013); <https://doi.org/10.1007/s10853-013-7438-y>
- [7] H. Bellakhder, A. Outzourhit, E.L Ameziane. Thin Solid Films. 382, 30 (2001); [https://doi.org/10.1016/S0040-6090\(00\)01697-7](https://doi.org/10.1016/S0040-6090(00)01697-7)
- [8] H. Singh, P. Singh, A. Thakur, T. Singh, J. Sharma. Materials Science in Semiconductor Processing. 75, 276 (2018); <https://doi.org/10.1016/j.mssp.2017.12.002>
- [9] E. Bacaksız, S. Aksu, N. Ozer, M. Tomakin, A. Ozcelik. Applied Surface Science. 256, 1566 (2009); <https://doi.org/10.1016/j.apsusc.2009.09.023>
- [10] S. Jeetendra, C. S. Naveen, P. Raghu, H. M. Mahesh. International Journal of Engineering Research & Technology. 3, 431 (2014).
- [11] A.K. S. Aqili, Z. Ali, A. Maqsood. Journal of Crystal Growth. 317, 47 (2011); <https://doi.org/10.1016/j.jcrysgro.2010.12.072>
- [12] A.K. S. Aqili, Z. Ali, A. Maqsood. Applied Surface Science. 167, 1 (2000); [https://doi.org/10.1016/S0169-4332\(00\)00498-0](https://doi.org/10.1016/S0169-4332(00)00498-0)
- [13] S. Jeetendra, H. Nagabhushana, K. Mrudula, C.S. Naveen, P. Raghu, H. M. Mahesh. Int. J. Electrochem. Sci. 9, 2944 (2014).
- [14] A. M. Salem, T. M. Dahy, Y. A. El-Gendy. Physica B: Condensed Matter 403, 3027 (2008); <https://doi.org/10.1016/j.physb.2008.03.005>

- [15] V. Kumar, V. Kumar, D. K. Dwivedi, (2012). *Physica Scripta*. 86, 015604 (2012); <https://doi.org/10.1088/0031-8949/86/01/015604>
- [16] A.B.M.O. Islam, N.B. Chaure, J. Wellings, G. Tolan, I.M. Dharmadasa. *Materials Characterization*. 60, 160 (2009); <https://doi.org/10.1016/j.matchar.2008.07.009>
- [17] K. R. Murali, M. Ziaudeen, N. Jayaprakash. *Solid-State Electronics* 50, 1692 (2006); <https://doi.org/10.1016/j.sse.2006.09.003>
- [18] W. Mahmood, S. Awan, A. Ud Din, J. Ali, M. F. Nasir, N. Ali, A. Haq, M. Kamran, B. Parveen, M. Rafiq, N. A. Shah. *Materials (Basel)*. 12, 1359 (2019); <https://doi.org/10.3390/ma12081359>
- [19] w. Mahmood, A. Thomas, A. ul Haq, N. A. Shah, M. F. Nasir. *Journal of Physics D: Applied Physics*. 50, 255503 (2017); <https://doi.org/10.1088/1361-6463/aa7157>
- [20] A. Aqili, A. J. Saleh, Z. Ali, Zulfiqar, S. Al-Omaria. *Journal of Alloys and Compounds*. 520,83 (2012); <https://doi.org/10.1016/j.jallcom.2011.12.094>
- [21] X. Li, D. W. Niles, F. S. Hasoon, R. J. Matson, P. Sheldon. *Journal of Vacuum Science & Technology A*. 17, 805 (1999); <https://doi.org/10.1116/1.581651>
- [22] A. K. S. Aqili, Z. Ali, S. Al-Omari, F. Afaneh. *Chalcogenide Letters*. 15(9),467 (2018).
- [23] A. Aqili, A. Maqsood, Z. Ali. *Applied Surface Science* 191,280 (2002); [https://doi.org/10.1016/S0169-4332\(02\)00218-0](https://doi.org/10.1016/S0169-4332(02)00218-0)
- [24] A. Aqili, A. Maqsood, *Applied optics*. 41, 218 (2002); <https://doi.org/10.1364/AO.41.000218>